BIOCHEMISTRY
including biophysical chemistry & molecular biology

Article

pubs.acs.org/biochemistry

Site-Directed Mutagenesis of Gln103 Reveals the Influence of This Residue on the Redox Properties and Stability of MauG

Sooim Shin,[†] Erik T. Yukl,[‡,§] Esha Sehanobish,[†] Carrie M. Wilmot,[‡] and Victor L. Davidson*[,†]

[†]Burnett School of Biomedical Sciences, College of Medicine, University of Central Florida, Orlando, Florida 32827, United States
[‡]Department of Biochemistry, Molecular Biology and Biophysics, University of Minnesota, Minneapolis, Minnesota 55455, United States

ABSTRACT: The diheme enzyme MauG catalyzes a six-electron oxidation that is required for the posttranslational modification of a precursor of methylamine dehydrogenase (preMADH) to complete the biosynthesis of its protein-derived cofactor, tryptophan tryptophylquinone (TTQ). Crystallographic and computational studies have implicated Gln103 in stabilizing the Fe^{IV}=O moiety of the bis-Fe^{IV} state by hydrogen bonding. The role of Gln103 was probed by site-directed mutagenesis. Q103L and Q103E mutations resulted in no expression and very little expression of the protein, respectively. Q103A MauG exhibited oxidative damage when isolated. Q103N MauG was isolated at levels comparable to that of wild-type MauG and exhibited normal activity in catalyzing the biosynthesis of TTQ from preMADH. The crystal structure of the Q103N MauG−preMADH complex suggests that a water may mediate hydrogen bonding between the shorter Asn103 side chain and the Fe^{IV}=O moiety. The Q103N mutation caused the two redox potentials associated with the diferric/diferrous redox couple to become less negative, although the redox cooperativity of the hemes of MauG was retained. Upon addition of H_2O_2, Q103N MauG exhibits changes in the absorbance spectrum in the Soret and near-IR regions consistent with formation of the bis-Fe^{IV} redox state. However, the rate of spontaneous return of the spectrum in the Soret region was 4.5-fold greater for Q103N MauG than for wild-type MauG. In contrast, the rate of spontaneous decay of the absorbance at 950 nm, which is associated with charge-resonance stabilization of the high-valence state, was similar for wild-type MauG and Q103N MauG. This suggests that as a consequence of the mutation a different distribution of resonance structures stabilizes the bis-Fe^{IV} state. These results demonstrate that subtle changes in the structure of the side chain of residue 103 can significantly affect the overall protein stability of MauG and alter the redox properties of the hemes.

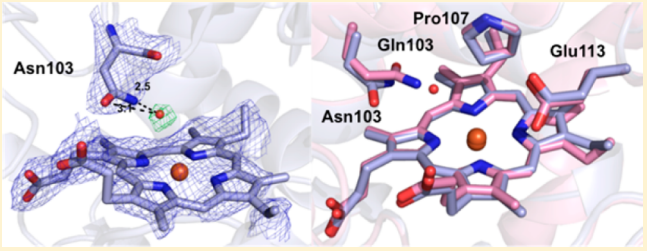

MauG from *Paracoccus denitrificans* is a 42 kDa *c*-type diheme enzyme[1] that catalyzes the final three two-electron oxidation reactions during the biosynthesis of the protein-derived cofactor,[2,3] tryptophan tryptophylquinone (TTQ).[4] TTQ is present in the enzyme methylamine dehydrogenase (MADH).[5] The substrate for MauG that undergoes this posttranslational modification is a precursor protein of MADH (preMADH). It possesses a monohydroxylated residue βTrp57[6,7] (Figure 1). The reactions catalyzed by MauG occur in the following order: covalent cross-linking of monohydroxylated βTrp57 to βTrp108, incorporation of a second oxygen atom into the side chain of βTrp57, and oxidation of the quinol species to the quinone.[8] Catalysis requires long-range electron transfer because preMADH does not make direct contact with either heme of MauG.[9] The electron transfer occurs via a hole-hopping mechanism[10] in which Trp residues of MauG are reversibly oxidized.[11−13]

High-valence Fe^{IV} species are important intermediates in the catalytic cycles of many heme enzymes. Many O_2-dependent and H_2O_2-dependent oxygenation mechanisms are believed to proceed via a ferric hydroperoxy intermediate.[14−17] This intermediate then loses water to yield Compound I, an Fe^{IV}=O species with a cation radical present on the π-porphyrin ring, or an amino acid axial ligand. Another common high-valence Fe species in heme proteins is Compound ES, an Fe^{IV}=O heme and amino acid-based radical in the proximity of the heme. The redox state of MauG that accepts electrons

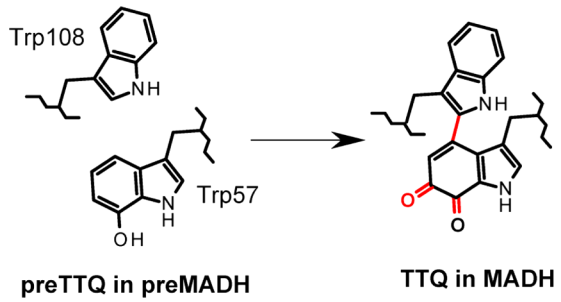

Figure 1. MauG-catalyzed biosynthesis of TTQ from preMADH. The post-translational modifications that are catalyzed by MauG are colored red.

Received: January 9, 2014
Revised: February 5, 2014
Published: February 11, 2014

dx.doi.org/10.1021/bi5000349 | *Biochemistry* 2014, 53, 1342−1349

during the oxidation of preMADH is bis-Fe^{IV},[18] with one heme an Fe^{IV}=O moiety with a His35 axial ligand and the other heme Fe^{IV} with axial heme ligands provided by His205 and Tyr294 side chains.[9] The bis-Fe^{IV} state is stabilized by MauG despite the fact that the two heme irons are separated by 21 Å.[9] Several structural features of MauG contribute to the formation and stabilization of the bis-Fe^{IV} state. Previous studies demonstrated that the axial ligand Tyr294 plays a critical role in stabilization of the Fe^{IV} state of the six-coordinate heme iron.[19−22] A tightly bound Ca^{2+} that is positioned in the proximity of the hemes was shown to influence the axial ligation geometry and magnetic properties of both hemes and consequently is required for activity.[23,24] Trp93, which resides between the two hemes, participates in an unusual charge-resonance transition that stabilizes the bis-Fe^{IV} state. The two Fe^{IV} hemes and Trp93 share spin and charge via very rapid hopping-mediated electron transfer.[13] In this model, the bis-Fe^{IV} state is the dominant species, but it is in charge resonance with an ensemble of resonance structures, including Compound ES-like and Compound I-like species.

Amino acid residues in the distal pocket of the high-spin heme also influence the formation and stabilization of this high-valence state. Mutagenesis studies of Glu113[25] indicated that the carboxyl group of Glu113 is an important determinant of the distribution of high-valence species that participate in charge-resonance stabilization of the bis-Fe^{IV} redox state, as well as in the maintenance of the redox cooperativity between the two hemes of MauG.[26] Pro107 is critical for maintaining the proper structure of the distal pocket of the high-spin heme of MauG, controlling the binding of exogenous ligands to the heme iron and directing the reactivity of the heme-activated oxygen during catalysis.[27] As a consequence of these roles, Pro107 minimizes the oxidation of other residues of MauG.[28] The diferrous MauG−NO structure[29] indicated a critical role for another residue, Gln103, as this residue interacts with the proximal nitrogen of bound NO via the donation of a hydrogen bond. This suggested that it might play a role in oxygen activation. Furthermore, a quantum chemical investigation of the spectroscopic parameters of the bis-Fe^{IV} MauG suggested that Gln103 is important in stabilizing the Fe^{IV}=O moiety by hydrogen bonding to the oxo ligand.[22] To determine the importance of Gln103 in the structure and function of MauG, this residue was converted to Ala, Leu, Glu, and Asn, and the consequences of these mutations are described.

EXPERIMENTAL PROCEDURES

Site-Directed Mutagenesis. Gln103 of MauG was converted to Ala, Asn, Leu, and Glu by site-directed mutagenesis of double-stranded pMEG391, which contains *mau*G, using the Phusion kit (New England Biolabs). The forward and reverse mutagenesis primers were 5′-CTGAAGCAAGCAGCCGGC-3′ and 5′-GTCGTCCGCCCGGC-3′ (Q103A), 5′-CTGAAGCAAGAAGCCGGC-3′ and 5′-GTCGTCCGCCCGGC-3′ (Q103E), 5′-CTGAAGCAAAACGCCGGC-3′ and 5′-GTCGTCCGCCCGGC-3′ (Q103N), and 5′-CTGAAGCAACTAGCCGGC-3′ and 5′-GTCGTCCGCCCGGC-3′ (Q103L), respectively. The codon for the residue that was mutated is underlined. The following thermal cycler conditions were employed: a 45 s, 98 °C initial denaturation step; a 20 s, 98 °C denaturation step; a 30 s, 68 °C primer annealing step; and a 270 s, 72 °C primer extension step. The plasmids were amplified in 25 cycles, and a 10 min, 72 °C final extension was performed.

Protein Expression and Purification. Previously described protocols were used for the purification of recombinant MauG from *P. denitrificans*[1] and preMADH from *Rhodobacter sphaeroides*.[6] Gln103 MauG variants were expressed in *P. denitrificans* and isolated from the periplasmic fraction as described for recombinant wild-type (WT) MauG.[1]

Mass Spectrometry. The Gln103 MauG variant proteins were analyzed by whole protein mass spectrometry. Samples were prepared and analyzed as described previously.[25] The data were obtained with a QSTAR XL (AB Sciex) quadrupole time-of-flight mass spectrometer with the IonSpray electrospray source, and Analyst QS version 1.0 (AB Sciex) and BioAnalyst extensions version 1.1 (AB Sciex) were used for the acquisition and analysis of the data.

Crystallization and X-ray Structure Determination of the Q103N MauG−preMADH Complex. Crystals of the Q103N MauG−preMADH complex were obtained using conditions similar to those used for crystallization of the WT MauG−preMADH complex.[9] X-ray diffraction data were collected at GM/CA-CAT beamline 23-ID-D of the Advanced Photon Source (APS) (Argonne National Laboratory, Argonne, IL). Data were collected at 100 K using a beam size matching the dimensions of the largest crystal face.

The diffraction data are essentially isomorphous with data obtained previously from crystals of the WT MauG−preMADH complex.[9] Data were processed with HKL2000,[30] and structure solutions were obtained by difference Fourier. The initial model used for building was that of the WT MauG−preMADH complex [Protein Data Bank (PDB) entry 3L4M] with solvent and ligands removed, and Gln103 mutated to Asn. Restrained refinement with TLS was conducted using REFMAC[31] in the CCP4 program suite,[32] and model building was conducted with COOT.[33] No distance restraints were used between the heme iron centers and their ligands. Refinement was deemed complete when the $F_o - F_c$ electron density contained only noise.

Redox Titrations. The E_m values of Q103 MauG variant proteins were determined by anaerobic spectrochemical titration, as described previously for WT MauG.[26] Data were fit by eq 1. This equation describes a system with two redox-active centers, where a is the fraction of the total absorbance change that can be attributed to one center and $1 - a$ is the fraction of the total absorbance change that can be attributed to the other.

$$\text{fraction reduced} = a/[1 + 10^{(E-E_{m1})/0.059\,V}] + (1 - a)/[1 + 10^{(E-E_{m2})/0.059\,V}] \quad (1)$$

Kinetic Studies. The steady-state kinetic parameters of the MauG-dependent biosynthesis of TTQ from preMADH were determined using a spectrophotometric assay, as previously described.[27,34] The data were fit by eq 2

$$v/E = k_{cat}[S]/([S] + K_m) \quad (2)$$

where S is preMADH and E is MauG. The electron transfer reaction from diferrous Q103N MauG to quinone MADH was studied by single-turnover kinetics as described previously for WT MauG.[35] Data were analyzed using eq 3

$$k_{obs} = k_{cat}[S]/([S] + K_d) \quad (3)$$

where S is quinone MADH.

dx.doi.org/10.1021/bi5000349 | *Biochemistry* 2014, 53, 1342−1349

RESULTS

Isolation and Purification of Gln103 MauG Variant Proteins. Gln103 was converted to Ala, Leu, Glu, and Asn by site-directed mutagenesis. The Q103L MauG variant was not detected in the expression system. Q103A, Q103N, and Q103E MauG variants were purified, and each protein migrated as a single band via sodium dodecyl sulfate−polyacrylamide gel electrophoresis at the same position as WT MauG. The yields of Q103A and Q103N MauG were each comparable to that of WT MauG. The yield of Q103E MauG was much smaller than that of WT MauG. Whole protein electrospray ionization mass spectrometry confirmed the identity of the isolated proteins. Q103E MauG and Q103N MauG each exhibited an observed mass that was consistent with the calculated mass within the resolution limit of the instrument. The Q103A MauG samples contained three species, one with the correct calculated mass, as well as significant proportions of +16 and +32 adducts. These same results were obtained for Q103A MauG from two different preparations. These results suggest that isolated Q103A MauG has undergone oxidative modification either *in vivo* or during the purification.

Effects of the Q103 Mutations on the Visible Absorption Spectra of the Diferric and Diferrous Redox States of MauG. The absorption spectra of the diferric Q103 MauG variants were compared to those of WT MauG. In WT MauG, the Soret peak is centered at 406 nm. The Q103E mutation causes a 4 nm red shift of the Soret peak maximum and a narrowing of the peak width relative to that of WT MauG (Figure 2A). The Q103A mutation causes a 2 nm red shift of the maximum with a narrowing of the Soret region (Figure 2B). The spectrum of Q103N MauG is similar to that of WT MauG except for a slight narrowing of the peak width (Figure 2C). The absorption spectra of the dithionite-reduced forms of the proteins were also compared (Figure 3). Reduction of WT MauG is characterized by an increase in the intensity of the Soret peak, a shift in the absorbance maximum to 418 nm, and the appearance of α and β bands at 550 and 520 nm, respectively. The spectra of the reduced Q103E and Q103N MauG variants were similar to that of WT MauG. The spectrum of reduced Q103A MauG was unusual. The Soret peak shifted but did not undergo an increase in intensity, and the normally small peak at 320 nm is greatly exaggerated.

X-ray Crystal Structure of Q103N MauG. Attempts were made to crystallize the Q103N, Q103A, and Q103E MauG variants, but only the Q103N MauG−preMADH complex yielded diffraction quality crystals. These were essentially isomorphous with the WT crystals, and the structure of the Q103N MauG−preMADH complex was determined to 2.6 Å (Table 1). The overall structures of WT and Q103N MauG−preMADH complexes are very similar with a root-mean-square deviation of 0.80 Å over the entire complex. Residual difference density in the high-spin heme distal pocket of Q103N was observed, consistent with the introduction of a water molecule within hydrogen bonding distance of Asn103 (Figure 4A). Although this hydrogen bond is shown between the water molecule and the nitrogen atom, the resolution of the data and the lack of definitive hydrogen bonding patterns do not preclude a 180° flip of the Asn103 side chain, placing the oxygen atom in hydrogen bond contact with water. Comparison of the high-spin heme environment of Q103N to that of WT MauG shows that other distal residues are largely

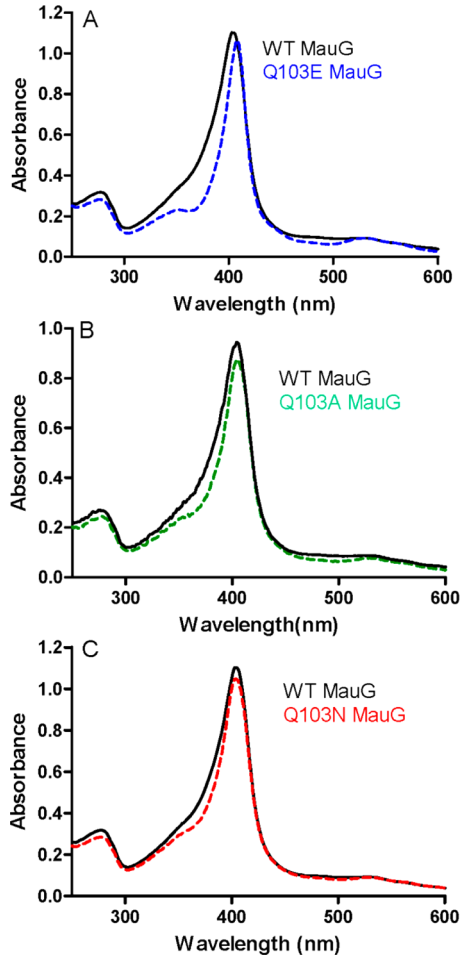

Figure 2. Comparison of the absorption spectra of diferric forms of WT with those of variant MauGs. (A) Overlay of the spectra of 3.5 μM diferric WT MauG (black) and Q103E MauG (blue). (B) Overlay of the spectra of 3.1 μM diferric WT MauG (black) and diferric Q103A MauG (green). (C) Overlay of the spectra of 3.5 μM diferric WT MauG (black) and Q103N MauG (red).

unperturbed by the mutation (Figure 4B). The water molecule introduced into the Q103N MauG structure adopts a position nearly coincident (within 1 Å) with the amide N atom of the Gln103 side chain in the WT structure. As Gln103 is proposed to be an important hydrogen bond donor stabilizing the bis-Fe(IV) state, this structure suggests that the water molecule introduced into the distal pocket of Q103N MauG is in a position to fulfill a similar function.

Effects of the Q103N Mutation on the Redox and Enzymatic Properties of MauG. Q103A MauG was isolated as a mixed population with a significant proportion of the protein exhibiting oxidative modification, as evidenced by mass spectrometry. The yield of Q103E MauG was very low, suggesting that this mutation significantly affected the biosynthesis of the protein, its stability, or both. Neither Q103A MauG nor Q103E MauG could be crystallized. For these reasons, the decision was made to focus the remaining studies on the Q103N MauG variant.

WT MauG exhibits two E_m values of −158 and −246 mV. These values correspond to the addition or removal of the first and second electrons from the diheme system.[34] The reductive titration of the as-isolated diferric Q103N yielded two E_m values of −11.2 ± 9.0 and −150.7 ± 5.9 mV (Figure 5). As in the case

dx.doi.org/10.1021/bi5000349 | *Biochemistry* 2014, 53, 1342−1349

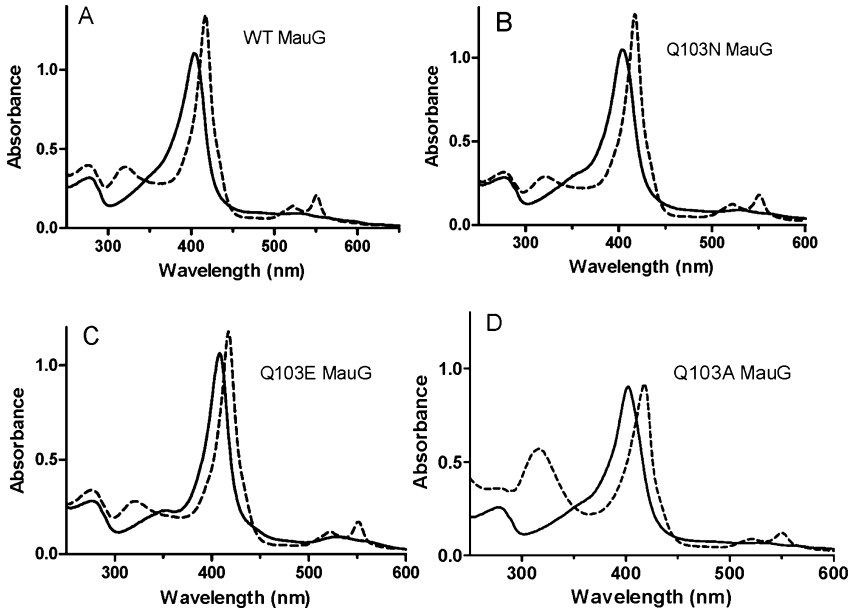

Figure 3. Comparison of the absorption spectra of oxidized and reduced forms of WT and Q103 variant MauGs. (A) Overlay of the spectra of 3.5 μM diferric WT MauG before (—) and after (---) reduction by sodium dithionite. (B) Overlay of the spectra of 3.5 μM diferric Q103N MauG before (—) and after (---) reduction by sodium dithionite. (C) Overlay of the spectra of 3.0 μM diferric Q103E MauG before (—) and after (---) reduction by sodium dithionite. (D) Overlay of the spectra of 3.5 μM diferric Q103A MauG before (—) and after (---) reduction by sodium dithionite.

of WT MauG, the two hemes of Q103N MauG were reduced simultaneously despite the two E_m values. Thus, the mutation did not disrupt the redox cooperativity between hemes that has been described for WT MauG,[26] but it did make the E_m values less negative.

A relatively stable bis-Fe^{IV} redox state is formed by addition of H_2O_2 to WT MauG as judged by changes in the Soret peak and near-infrared (NIR) region of the absorbance spectrum.[13,18] It exhibits a decrease in the intensity of the Soret peak and a 2 nm red shift of the absorption maxima (Figure 6A), as well as the appearance of a broad absorbance centered at 950 nm (Figure 6B). The latter feature is characteristic of a charge-resonance transition that stabilizes the bis-Fe^{IV} state.[13] Reaction of Q103N MauG with H_2O_2 caused similar but not identical spectral changes. Whereas WT MauG displays a red shift of both sides of the Soret peak, Q103N MauG displays a sharper peak caused by a red shift for only the lower-wavelength side of the Soret band (Figure 6C). As seen with WT MauG, a peak centered at 950 nm also appears. The intensity of the α/β bands, which present as two peaks in the 520−560 nm region, is decreased in Q103N MauG, and it exhibits some weak absorbance in the 600−700 nm region (Figure 6D). For WT MauG, the spontaneous return of the spectrum to that of the diferric state occurs over several minutes, with the changes in the Soret and NIR regions occurring at similar rates.[13] However, the H_2O_2-induced spectral changes in the Soret and NIR regions of the Q103N MauG spectrum spontaneously decayed at different rates. The rate of change in the Soret peak of Q103N MauG [k = (1.4 ± 0.1) × 10^{-2} s^{-1}] is 4.5-fold greater than for WT MauG [k = (3.1 ± 0.3) × 10^{-3} s^{-1}] (Figure 6E). In contrast, the rates of decay of the peak at 950 nm for WT MauG [k = (1.7 ± 0.1) × 10^{-3} s^{-1}] and Q103N MauG [k = (2.5 ± 0.4) × 10^{-3} s^{-1}] are similar (Figure 6F).

The steady-state kinetic parameters of Q103N MauG-dependent TTQ biosynthesis were determined using preMADH and H_2O_2 as the substrates (Figure 7A). WT MauG exhibited a k_{cat} of 0.16 ± 0.1 s^{-1} and a K_m of 2.0 ± 0.3 μM for preMADH. Q103N MauG exhibited a k_{cat} of 0.14 ± 0.1 s^{-1} and a K_m of 2.1 ± 0.3 μM for preMADH. In addition to this biosynthetic reaction, a nonbiosynthetic electron transfer reaction from diferrous MauG to quinone MADH has been characterized.[35] This reaction does not require formation of the bis-Fe^{IV} state. Q103N MauG was active in this electron transfer reaction (Figure 7B) and exhibited a rate constant of 0.053 ± 0.004 s^{-1} and a K_d of 6.2 ± 1.7 μM. WT MauG exhibited a rate constant of 0.063 ± 0.002 s^{-1} and a K_d of 10.4 ± 0.8 μM. The decreased reaction rate could be a consequence of the fact that the Q103N mutation makes the E_m values associated with the diferric/diferrous MauG couple ∼100 mV less negative. This would decrease the thermodynamic driving force for this electron transfer reaction. Unfortunately, it was not possible to determine the E_m values associated with the bis-Fe^{IV}/diferric couple. It should be noted that even if these E_m values were affected by the mutation, an effect on the steady-state rate of biosynthesis of TTQ from preMADH might not be observed because the steady-state k_{cat} is approximately 4-fold lower than the rate constant for the reduction of bis-Fe^{IV} in WT MauG by preMADH.[34,36]

■ DISCUSSION

Gln103 is one of three residues in the distal pocket of the high-spin heme of MauG. This residue has been implicated in catalytic activity on the basis of crystal structures of the MauG−preMADH complex[9] and the NO adduct of MauG.[29] Pro107 was shown to be critical for maintaining the proper structure around the high-spin heme, controlling O_2 or H_2O_2 binding, and directing the reactivity of the resulting high-valence intermediate toward productive catalysis rather than oxidative damage.[27,28] Glu113 was shown to be required for the formation and stabilization of both the diferrous and bis-Fe^{IV} redox states of MauG.[25] The results of this study provide

dx.doi.org/10.1021/bi5000349 | Biochemistry 2014, 53, 1342−1349

Table 1. X-ray Crystallography Data Collection and Refinement Statistics for the Q103N MauG−preMADH Complex[a]

Data Collection	
space group	*P*1
unit cell lengths (Å)	55.90 × 86.02 × 108.08
unit cell angles (deg)	111.52, 91.75, 104.22
wavelength (Å)	1.03324
resolution (Å)	50.00−2.59 (2.63−2.59)[a]
no. of measured reflections	211579
no. of unique reflections	55071
completeness (%)	98.6 (97.6)
R_{merge} (%)[b]	11.5 (59.9)
$I/\sigma I$	12.4 (2.1)
multiplicity	3.8 (3.8)
Refinement	
R_{work} (%)[c]	19.8
R_{free} (%)[d]	25.4
no. of protein atoms	13269
no. of ligand atoms	222
no. of solvent atoms	398
Ramachandran statistics[e] (%)	
allowed	98.89
outliers	1.01
root-mean-square deviation	
bond lengths (Å)	0.005
bond angles (deg)	1.400
average *B* factor (Å^2)	52.60
PDB entry	4O1Q

[a]Values in parentheses are for the highest-resolution shell. [b]$R_{merge} = \sum_i|I_{hkl,i} - \langle I_{hkl}\rangle|/\sum_{hkl}\sum_i I_{hkl,i}$, where I is the observed intensity and $\langle I_{hkl}\rangle$ is the average intensity of multiple measurements. [c]$R_{work} = \sum||F_o| - |F_c||/\sum|F_o|$, where F_o is the observed structure factor amplitude and F_c is the calculated structure factor amplitude. [d]R_{free} is the R factor based on 5% of the data excluded from refinement. [e]Based on values attained from refinement validation options in COOT.

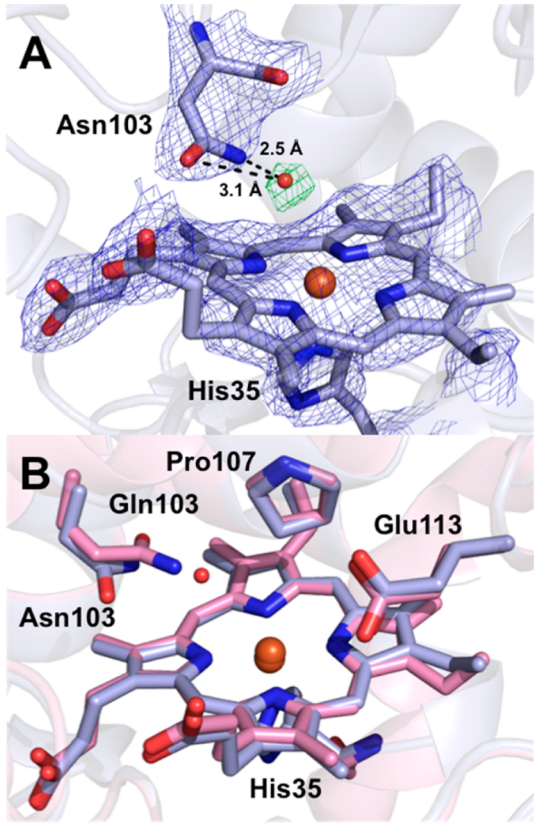

Figure 4. (A) Electron density for the high-spin heme and Q103N mutation site in MauG from the Q103N MauG−preMADH crystal structure, showing difference density for a model without the water molecule within hydrogen bond distance of Asn103. The $2F_o - F_c$ density is drawn as blue mesh contoured at 1.0σ. Positive $F_o - F_c$ density is drawn as green mesh contoured at 4.0σ. (B) Comparison of the Q103N (blue) and WT (PDB entry 3L4M, pink) MauG high-spin hemes and distal residues. This figure was generated using Pymol (http://www.pymol.org/).

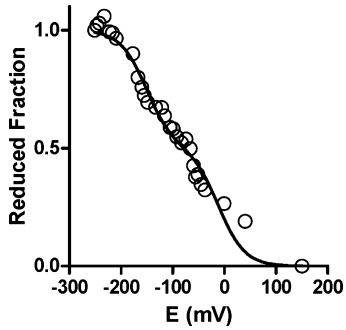

Figure 5. Spectrochemical redox titration of Q103N MauG. The titration was performed anaerobically in 50 mM potassium phosphate (pH 7.5) at 25 °C. The fraction of MauG that was reduced was determined by comparison with the spectra of the completely oxidized and reduced forms of MauG and quantitated from the absorbance at 550 nm. The solid line is the fit of the data to eq 1.

insight into the role of Gln103, which has been postulated to be important in stabilizing the Fe^{IV}=O moiety of the bis-Fe^{IV} intermediate through hydrogen bonding.[22,29]

The importance of residue Gln103 is highlighted by the observation that nonconservative mutations at this position are not well-tolerated. While near-WT levels of Q103N MauG could be isolated, Q103L MauG was undetectable and Q103E MauG could be isolated in only small amounts insufficient for detailed studies. Although sterically conservative, these mutations alter the electrostatic environment of the heme and adversely affect the biosynthesis of the MauG protein, its stability, or both. The observation that isolated Q103A MauG has undergone oxidative modification could be explained by either a decreased level of stabilization of the bis-Fe^{IV} state or the generation of an alternative high-valence heme species that leads to nonspecific oxidation of nearby residues. A similar phenomenon was observed as a consequence of certain mutations of Pro107, which is positioned near Gln103 (see Figure 4B).[27,28]

The Q103N mutation makes the E_m values associated with the diferric/diferrous couple ~100 mV less negative. This could be due to altered hydrogen bonding networks that stabilize the reduced state of Q103N MauG relative to WT MauG. It was previously shown that an E113Q mutation also altered this redox couple; however, in that case, the redox cooperativity between the hemes was abolished,[25] whereas the cooperativity is retained in Q103N MauG. A notable effect of the Q103N mutation is on the nature and stability of the high-valence species that is formed upon reaction with H_2O_2. The spectral changes that are observed initially upon reaction with H_2O_2 are very similar to those of WT MauG and consistent with formation of the bis-Fe^{IV} state. However, the spontaneous return to the resting spectrum of the Soret peak is 4.5-fold

dx.doi.org/10.1021/bi5000349 | *Biochemistry* 2014, 53, 1342−1349

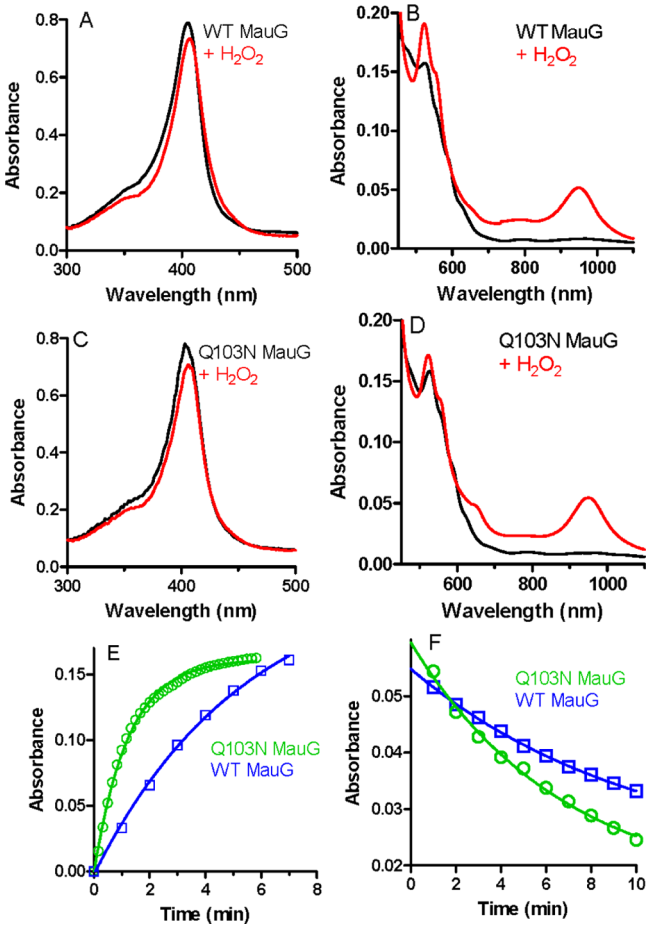

Figure 6. Changes in absorption spectra of WT and Q103N MauG after addition of H_2O_2. Panels A–D display overlays of the Soret region (A) and NIR region (B) of the spectrum of 2.5 μM diferric WT MauG before (black line) and immediately after (red line) addition of a stoichiometric amount of H_2O_2, and of the Soret region (C) and NIR region (D) of the spectrum of 2.5 μM diferric Q103N MauG before (black line) and immediately after (red line) addition of a stoichiometric amount of H_2O_2. (E) Time course for the return to the resting spectrum of WT MauG (blue squares) and Q103N MauG (green circles) in the Soret region. This describes the transition from the red spectrum back to the black spectrum in panels A and C. The data are for the absorbance at 405 nm for WT MauG and 403 nm for Q103N MauG. The lines are the fits of each data set to a single-exponential transition. (F) Time course for the return to the resting spectrum of WT MauG (blue squares) and Q103N MauG (green circles) in the NIR region. This describes the transition from the red spectrum back to the black spectrum in panels B and D. The data are for the absorbance at 950 nm. The lines are the fits of each data set to a single-exponential transition.

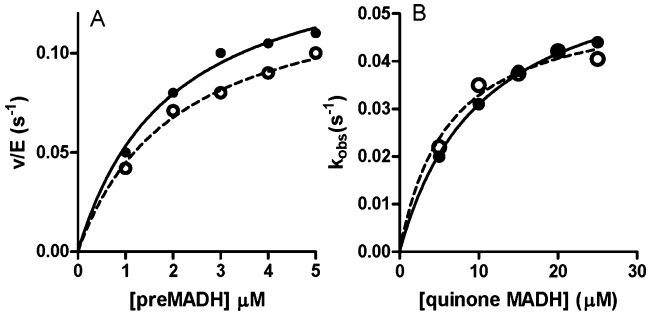

Figure 7. Steady-state and single-turnover kinetic analysis. (A) Steady-state kinetics of Q103N MauG-dependent (○) and WT MauG-dependent (●) biosynthesis of TTQ from preMADH. MauG was mixed with preMADH in 0.01 M potassium phosphate buffer (pH 7.5) at 25 °C. Reactions were initiated by the addition of 100 μM H_2O_2, and the rate of appearance of quinone MADH was monitored at 440 nm. The lines are fits of the data to eq 2. (B) Single-turnover kinetics of the reaction of diferrous Q103N MauG (○) and WT MauG (●) with quinone MADH. Reaction mixtures contained a fixed concentration of diferrous MauG (1.25 μM) and varied concentrations of quinone MADH. The reaction was monitored by the decrease in absorbance at 550 nm that corresponds to the conversion of diferrous to diferric MauG. The data for the concentration dependence of the rate are fit to eq 3.

greater than that observed for WT MauG. In contrast, the decay of the NIR peak occurs at a rate similar to that of WT MauG.

The NIR absorbance of the bis-Fe^{IV} state has been attributed to an unusual charge-resonance transition in which the two Fe^{IV} hemes and Trp93 share spin and charge via very rapid hopping-mediated electron transfer.[13] In this model, the bis-Fe^{IV} state is the dominant species, but it is in charge resonance with an ensemble of resonance structures, including Compound ES-like and Compound I-like species. It was previously shown that E113Q MauG exhibited the NIR absorbance feature but did not exhibit the characteristic change in the Soret peak.[25] The explanation for those results was that the E113Q mutation altered the distribution of resonance structures such that the bis-Fe^{IV} state was no longer the dominant species within the ensemble and therefore existed for only a small percentage of the time. This unfavorable resonance equilibrium for bis-Fe^{IV} stabilization limited the availability of the bis-Fe^{IV} state, consistent with the observed loss of activity that was caused by the E113Q mutation. In contrast, with Q103N MauG, it appears that a bis-Fe^{IV} state with a distribution of resonance structures similar to WT MauG initially forms. However, the subsequent more rapid change in the Soret peak without a concomitant change in the 950 nm absorbance suggests that one or more of the high-valence species predominantly associated with the changes in the Soret peak, but not the NIR feature, decay more quickly or alternatively are converted to a different high-valence species that allows retention of the charge-resonance stabilization. The presence of a different ensemble of resonance structures stabilizing the bis-Fe^{IV} state in Q103N MauG could also explain the subtle differences in absorbance features in the 520–700 nm region of the spectrum (see Figure 6). This could be a consequence of a subtle difference in the stability of the ferryl heme and other high-valence species because of the differential hydrogen bonding to a water rather than the Gln103 side chain. In contrast to what was seen with the E113Q mutation, the bis-Fe^{IV} state of Q103N is still the dominant species among the resonance structures, and this allows normal reactivity toward preMADH.

These results are consistent with the hypothesis that Gln103 is important in the stabilization of the Fe^{IV}=O moiety by hydrogen bonding to the oxo. Even though Asn103 is unable to directly form a hydrogen bond with the ferryl heme moiety in Q103N MauG, the high-valence species is still relatively stable. The reason that its lifetime is not more transient as a consequence of this mutation may be explained by the crystal structure, which supports the proposal that a water forms a bridge between the shorter Asn103 side chain and the Fe^{IV}=O moiety through hydrogen bonding. The hydrogen bond to the oxo iron ligand may be weaker than the direct hydrogen bond

dx.doi.org/10.1021/bi5000349 | *Biochemistry* 2014, 53, 1342–1349

to Gln103 observed in WT MauG. This could explain the initial change in the Soret peak leading to a different distribution of resonance structures that contribute to charge-resonance stabilization of the bis-Fe^{IV} state. These results and those of previous studies[19,25,37] indicate that multiple amino acid residues surrounding the hemes of MauG actively participate in controlling the stabilization of the charge-resonance stabilization of the high-valence state of MauG. The deleterious effects of replacement of Gln103 with Leu or Glu, and the oxidative damage observed upon replacement with Ala, coupled with an inability to crystallize these variants, further speak to the importance of residue Gln103 in the overall stability of the MauG protein, as well as control of the reactivity of the hemes.

■ ASSOCIATED CONTENT

Accession Codes

The coordinates and structure factors for the Q103N MauG−preMADH complex have been deposited in the PDB as entry 4O1Q.

■ AUTHOR INFORMATION

Corresponding Author

*E-mail: victor.davidson@ucf.edu. Telephone: (407) 266-7111. Fax: (407) 266-7002.

Present Address

[§]E.T.Y.: Department of Chemistry and Biochemistry, New Mexico State University, Las Cruces, NM 88003.

Funding

This research was supported by National Institute of General Medical Sciences Grants R37GM41574 (V.L.D.), R01GM66569 (C.M.W.), and F32GM97779 (E.T.Y.) and Minnesota Partnership for Biotechnology and Medical Genomics Grant SPAP-05-0013-P-FY06 (C.M.W.).

Notes

The authors declare no competing financial interest.

■ ACKNOWLEDGMENTS

Computer resources were provided by the Basic Sciences Computing Laboratory of the University of Minnesota Supercomputing Institute, and we thank Nancy Rowe for her support. X-ray data were collected at the Kahlert Structural Biology Laboratory (KSBL) at The University of Minnesota and GM/CA-CAT at the APS. GM/CA CAT has been funded with funds from the National Cancer Institute (Y1-CO-1020) and the National Institute of General Medical Sciences (Y1-GM-1104). Use of the APS was supported by the U.S. Department of Energy, Basic Energy Sciences, Office of Science, under Contract DE-AC02-06CH11357. We thank Ed Hoeffner for KSBL support and the staff at Sector 23 of the APS for their support. We also thank Yu Tang for technical assistance.

■ ABBREVIATIONS

TTQ, tryptophan tryptophylquinone; preMADH, biosynthetic precursor protein of MADH with incompletely synthesized TTQ; bis-Fe(IV) MauG, redox state of MauG with one heme as Fe(IV)═O and the other as Fe(IV); WT, wild-type; NIR, near-infrared.

■ REFERENCES

(1) Wang, Y., Graichen, M. E., Liu, A., Pearson, A. R., Wilmot, C. M., and Davidson, V. L. (2003) MauG, a novel diheme protein required for tryptophan tryptophylquinone biogenesis. *Biochemistry 42*, 7318−7325.

(2) Davidson, V. L. (2007) Protein-derived cofactors. Expanding the scope of post-translational modifications. *Biochemistry 46*, 5283−5292.

(3) Davidson, V. L. (2011) Generation of protein-derived redox cofactors by posttranslational modification. *Mol. BioSyst. 7*, 29−37.

(4) McIntire, W. S., Wemmer, D. E., Chistoserdov, A., and Lidstrom, M. E. (1991) A new cofactor in a prokaryotic enzyme: Tryptophan tryptophylquinone as the redox prosthetic group in methylamine dehydrogenase. *Science 252*, 817−824.

(5) Davidson, V. L. (2001) Pyrroloquinoline quinone (PQQ) from methanol dehydrogenase and tryptophan tryptophylquinone (TTQ) from methylamine dehydrogenase. *Adv. Protein Chem. 58*, 95−140.

(6) Pearson, A. R., De La Mora-Rey, T., Graichen, M. E., Wang, Y., Jones, L. H., Marimanikkupam, S., Agger, S. A., Grimsrud, P. A., Davidson, V. L., and Wilmot, C. M. (2004) Further insights into quinone cofactor biogenesis: Probing the role of *mauG* in methylamine dehydrogenase tryptophan tryptophylquinone formation. *Biochemistry 43*, 5494−5502.

(7) Davidson, V. L., and Wilmot, C. M. (2013) Posttranslational biosynthesis of the protein-derived cofactor tryptophan tryptophylquinone. *Annu. Rev. Biochem. 82*, 531−550.

(8) Yukl, E. T., Liu, F., Krzystek, J., Shin, S., Jensen, L. M., Davidson, V. L., Wilmot, C. M., and Liu, A. (2013) Diradical intermediate within the context of tryptophan tryptophylquinone biosynthesis. *Proc. Natl. Acad. Sci. U.S.A. 110*, 4569−4573.

(9) Jensen, L. M., Sanishvili, R., Davidson, V. L., and Wilmot, C. M. (2010) In crystallo posttranslational modification within a MauG/pre-methylamine dehydrogenase complex. *Science 327*, 1392−1394.

(10) Giese, B., Graber, M., and Cordes, M. (2008) Electron transfer in peptides and proteins. *Curr. Opin. Chem. Biol. 12*, 755−759.

(11) Abu Tarboush, N., Jensen, L. M. R., Yukl, E. T., Geng, J., Liu, A., Wilmot, C. M., and Davidson, V. L. (2011) Mutagenesis of tryptophan199 suggets that hopping is required for MauG-dependent tryptophan tryptophylquinone biosynthesis. *Proc. Natl. Acad. Sci. U.S.A. 108*, 16956−16961.

(12) Choi, M., Shin, S., and Davidson, V. L. (2012) Characterization of electron tunneling and hole hopping reactions between different forms of MauG and methylamine dehydrogenase within a natural protein complex. *Biochemistry 51*, 6942−6949.

(13) Geng, J., Dornevil, K., Davidson, V. L., and Liu, A. (2013) Tryptophan-mediated charge-resonance stabilization in the bis-Fe(IV) redox state of MauG. *Proc. Natl. Acad. Sci. U.S.A. 110*, 9639−9644.

(14) Groves, J. T. (2006) High-valent iron in chemical and biological oxidations. *J. Inorg. Biochem. 100*, 434−447.

(15) Hiner, A. N., Raven, E. L., Thorneley, R. N., Garcia-Canovas, F., and Rodriguez-Lopez, J. N. (2002) Mechanisms of compound I formation in heme peroxidases. *J. Inorg. Biochem. 91*, 27−34.

(16) Shaik, S., de Visser, S. P., and Kumar, D. (2004) One oxidant, many pathways: A theoretical perspective of monooxygenation mechanisms by cytochrome P450 enzymes. *JBIC, J. Biol. Inorg. Chem. 9*, 661−668.

(17) Sono, M., Roach, M. P., Coulter, E. D., and Dawson, J. H. (1996) Heme-containing oxygenases. *Chem. Rev. 96*, 2841−2888.

(18) Li, X., Fu, R., Lee, S., Krebs, C., Davidson, V. L., and Liu, A. (2008) A catalytic di-heme bis-Fe(IV) intermediate, alternative to an Fe(IV)═O porphyrin radical. *Proc. Natl. Acad. Sci. U.S.A. 105*, 8597−8600.

(19) Abu Tarboush, N., Jensen, L. M., Feng, M., Tachikawa, H., Wilmot, C. M., and Davidson, V. L. (2010) Functional importance of tyrosine 294 and the catalytic selectivity for the bis-Fe(IV) state of MauG revealed by replacement of this axial heme ligand with histidine. *Biochemistry 49*, 9783−9791.

(20) Abu Tarboush, N., Shin, S., Geng, J., Liu, A., and Davidson, V. L. (2012) Effects of the loss of the axial tyrosine ligand of the low-spin heme of MauG on its physical properties and reactivity. *FEBS Lett. 586*, 4339−4343.

(21) Jensen, L. M., Meharenna, Y. T., Davidson, V. L., Poulos, T. L., Hedman, B., Wilmot, C. M., and Sarangi, R. (2012) Geometric and

electronic structures of the His-Fe(IV)═O and His-Fe(IV)-Tyr hemes of MauG. *JBIC, J. Biol. Inorg. Chem. 17*, 1241−1255.
(22) Ling, Y., Davidson, V. L., and Zhang, Y. (2010) Unprecedented Fe(IV) species in a diheme protein MauG: A quantum chemical investigation on the unusual Mössbauer spectroscopic properties. *J. Phys. Chem. Lett. 1*, 2936−2939.
(23) Chen, Y., Naik, S. G., Krzystek, J., Shin, S., Nelson, W. H., Xue, S., Yang, J. J., Davidson, V. L., and Liu, A. (2012) Role of calcium in metalloenzymes: Effects of calcium removal on the axial ligation geometry and magnetic properties of the catalytic diheme center in MauG. *Biochemistry 51*, 1586−1597.
(24) Shin, S., Feng, M. L., Chen, Y., Jensen, L. M. R., Tachikawa, H., Wilmot, C. M., Liu, A., and Davidson, V. L. (2011) The tightly bound calcium of MauG is required for tryptophan tryptophylquinone cofactor biosynthesis. *Biochemistry 50*, 144−150.
(25) Abu Tarboush, N., Yukl, E. T., Shin, S., Feng, M., Wilmot, C. M., and Davidson, V. L. (2013) Carboxyl group of Glu113 is required for stabilization of the diferrous and bis-Fe(IV) states of MauG. *Biochemistry 52*, 6358−6367.
(26) Li, X., Feng, M., Wang, Y., Tachikawa, H., and Davidson, V. L. (2006) Evidence for redox cooperativity between *c*-type hemes of MauG which is likely coupled to oxygen activation during tryptophan tryptophylquinone biosynthesis. *Biochemistry 45*, 821−828.
(27) Feng, M., Jensen, L. M., Yukl, E. T., Wei, X., Liu, A., Wilmot, C. M., and Davidson, V. L. (2012) Proline 107 is a major determinant in maintaining the structure of the distal pocket and reactivity of the high-spin heme of MauG. *Biochemistry 51*, 1598−1606.
(28) Yukl, E. T., Williamson, H. R., Higgins, L., Davidson, V. L., and Wilmot, C. M. (2013) Oxidative Damage in MauG: Implications for the Control of High-Valent Iron Species and Radical Propagation Pathways. *Biochemistry 52*, 9447−9455.
(29) Yukl, E. T., Goblirsch, B. R., Davidson, V. L., and Wilmot, C. M. (2011) Crystal structures of CO and NO adducts of MauG in complex with pre-methylamine dehydrogenase: Implications for the mechanism of dioxygen activation. *Biochemistry 50*, 2931−2938.
(30) Otwinowski, Z., and Minor, W. (1997) Processing of X-ray diffraction data collected in oscillation mode. *Methods Enzymol. 276*, 307−326.
(31) Murshudov, G. N., Vagin, A. A., and Dodson, E. J. (1997) Refinement of macromolecular structures by the maximum-likelihood method. *Acta Crystallogr. D53*, 240−255.
(32) Collaborative Computational Project Number 4 (1994) The CCP4 suite: Programs for protein crystallography. *Acta Crystallogr. D50*, 760−763.
(33) Emsley, P., and Cowtan, K. (2004) Coot: Model-building tools for molecular graphics. *Acta Crystallogr. D60*, 2126−2132.
(34) Li, X., Jones, L. H., Pearson, A. R., Wilmot, C. M., and Davidson, V. L. (2006) Mechanistic possibilities in MauG-dependent tryptophan tryptophylquinone biosynthesis. *Biochemistry 45*, 13276−13283.
(35) Shin, S., Abu Tarboush, N., and Davidson, V. L. (2010) Long-range electron transfer reactions between hemes of MauG and different forms of tryptophan tryptophylquinone of methylamine dehydrogenase. *Biochemistry 49*, 5810−5816.
(36) Lee, S., Shin, S., Li, X., and Davidson, V. L. (2009) Kinetic mechanism for the initial steps in MauG-dependent tryptophan tryptophylquinone biosynthesis. *Biochemistry 48*, 2442−2447.
(37) Shin, S., Feng, M., and Davidson, V. L. (2013) Mutation of Trp(93) of MauG to tyrosine causes loss of bound Ca^{2+} and alters the kinetic mechanism of tryptophan tryptophylquinone cofactor biosynthesis. *Biochem. J. 456*, 129−137.